



BIOMARKERS, GENOMICS, PROTEOMICS, AND GENE REGULATION

miR-135b Coordinates Progression of ErbB2-Driven Mammary Carcinomas through Suppression of MID1 and MTCH2

Maddalena Arigoni,^{*} Giuseppina Barutello,^{*} Federica Riccardo,^{*} Elisabetta Ercole,^{*} Daniela Cantarella,[†] Francesca Orso,^{*} Laura Conti,^{*} Stefania Lanzardo,^{*} Daniela Taverna,^{*} Irene Merighi,^{*} Raffaele A. Calogero,^{*‡} Federica Cavallo,^{*} and Elena Quaglinò^{*}

From the Department of Molecular Biotechnology and Health Sciences,^{*} Molecular Biotechnology Center, the Department of Oncological Sciences,[†] Institute for Cancer Research and Treatment, and the CIR Molecular Systems Biology,[‡] University of Torino, Torino, Italy

Accepted for publication
February 28, 2013.

Address correspondence to
Raffaele A. Calogero, D.Sc.,
Molecular Biotechnology
Center, University of Torino,
Via Nizza 52, 10126 Torino,
Italy. E-mail: raffaele.calogero@unito.it.

In an attempt to reveal deregulated miRNAs associated with the progression of carcinomas developed in BALB-neuT transgenic mice, we found increased expression of miR-135b during malignancy. Relevantly, we observed that miR-135b is up-regulated in basal or normal-like human breast cancers, and it correlates with patient survival and early metastatization. Therefore, we investigated its biological functions by modulating its expression (up- or down-regulation) in mammary tumor cells. Although no effect was observed on proliferation in cell culture and in orthotopically injected mice, miR-135b was able to control cancer cell stemness in a mammosphere assay, anchorage-independent growth *in vitro*, and lung cancer cell dissemination in mice after tail vein injections. Focusing on the miR-135b molecular mechanism, we observed that miR-135b controls malignancy via its direct targets, midline 1 (MID1) and mitochondrial carrier homolog 2 (MTCH2), as proved by biochemical and functional rescuing/phenocopying experiments. Consistently, an anti-correlation between miR-135b and MID1 or MTCH2 was found in human primary tumor samples. In conclusion, our research led us to the identification of miR-135b and its targets, MID1 and MTCH2, as relevant coordinators of mammary gland tumor progression. (*Am J Pathol* 2013, 182: 2058–2070; <http://dx.doi.org/10.1016/j.ajpath.2013.02.046>)

Breast cancer is one of the major health problems of the Western world.¹ Although the survival rate has improved with progress in screening and adjuvant therapies, one third of the patients present cancer recurrences 10 years after the diagnosis.² More than 90% of mortality from cancer is attributable to metastases and not to the primary tumor from which metastases arise.³ Identification of the genetic and epigenetic changes foreshadowing metastasis is, thus, one of the highest priorities for translational cancer research. Although several protein-coding genes involved in malignancy have been identified and characterized,⁴ noncoding genes, such as miRNAs that have been shown to regulate many aspects of the metastatic process, have to be characterized.⁵ Several clinical studies show a correlation between miRNA expression and recurrence, development of metastasis, and/or survival.⁶ miRNAs may also contribute to the metastatic program by modulating the structure of the tumor microenvironment, influencing the ability of cancer cells to move and survive.⁷ Moreover, miRNAs are involved in the

maintenance of the cancer stem cell (CSC) phenotype by connecting stemness and metastasis through regulation of epithelial-to-mesenchymal transition.⁸ Global miRNA deregulation has been shown in breast cancer,^{9–12} whereas specific miRNAs have been associated with clinicopathological features of breast tumors, such as estrogen and progesterone receptor expression,¹³ tumor grade,¹⁰ vascular invasion, or proliferation index.¹⁴ As far as breast cancer is concerned, among other findings, reduced expression of miR-145,¹⁵ miR-335,¹⁶ and miR-126,¹⁷ and overexpression of miR-10b,¹⁸ miR-21,¹⁹ and miR-210²⁰ were significantly associated with breast cancer invasion and metastasis.

Supported by grants from the Associazione Italiana per la Ricerca sul Cancro (IG 5377), the Italian Ministry for the Universities and Research (PRIN 2008W3KW2A, PRIN, and FIRB Giovani RBFR08F2FS-002 FO), the Regione Piemonte (Piattaforma Innovativa Biotecnologie per le Scienze della Vita, ImmOnc project), and Epigenomics Flagship Project EPIGEN, MIUR-CNR.

F.C. and E.Q. contributed equally to this work as senior authors.

However, profiling studies have been mainly focused on miRNAs deregulated in primary breast cancer^{12,21} or in breast cancer cell lines.²² By contrast, characterization of a deregulated miRNA expression profile during carcinogenesis progression would permit assessment of their involvement in tumor development and the efficacy of miRNA targeting during tumor progression.

BALB-neuT mice are a realistic model of mammary cancer, because all females develop invasive and metastatic rat ErbB2⁺ mammary carcinomas, with a stepwise progression similar to that of women.^{23,24} As in several cases of human mammary cancer, systemic metastatization is an early event in BALB-neuT carcinogenesis.²⁵ Moreover, the gene expression pattern associated with cancer progression reveals major similarities with human ErbB2⁺ breast carcinomas.^{26,27} In this study, we show that miR-135a and miR-135b are strongly up-regulated in invasive carcinomas of BALB-neuT mice compared with normal mammary tissue. Down-modulation of miR-135b in cancer cells from BALB-neuT mice revealed its major role in anchorage-independent growth and lung metastasis formation. MID1 and MTCH2 were also identified and validated as putative miR-135b targets.

Materials and Methods

Mice

Female BALB/c and rat ErbB2 transgenic BALB-neuT mice²⁸ were bred by Biogem IRGS (Ariano Irpino, Italy), maintained in the transgenic unit of the Molecular Biotechnology Center (University of Torino, Torino, Italy) under a 12-hour light-dark cycle, and provided food and water ad libitum. Mice were treated in conformity with European laws and policies,²⁹ and this study was approved by the Ethical Committee of the University of Torino.

Cell Lines and Mammosphere Culture

BALB-neuT line 1 (TUBO cells),³⁰ BALB-neuT line 2, and BALB-neuT line 3 are derived from autochthonous ErbB2⁺ mammary carcinomas arising in BALB-neuT female mice. They were cultured in Dulbecco's modified Eagle's medium with Glutamax 1 (Life Technologies, Monza, Italy), supplemented with 20% heat-inactivated fetal bovine serum (Invitrogen, Carlsbad, CA) (complete medium). TSA (a highly aggressive and metastatizing cell line established from a moderately differentiated mammary adenocarcinoma that arose spontaneously in a BALB/c mouse)³¹ and 4T1 (mouse breast cancer cells sourced from ATCC, Manassas, VA) cell lines were maintained in RPMI 1640 medium (Life Technologies), supplemented with 10% heat-inactivated fetal bovine serum (Invitrogen). TUBO, TSA, and 4T1 cells were grown in adherent conditions as an epithelial monolayer in mammosphere medium (serum-free Dulbecco's modified Eagle's medium—F12 medium supplemented with 20 ng/mL basic fibroblast growth factor, 20 ng/mL epidermal growth

factor, 5 µg/mL insulin, and 0.4% bovine serum albumin; all from Sigma-Aldrich, Milano, Italy) to generate E cells.

TUBO cells were dissociated enzymatically and mechanically, using trypsin and pipetting, and were plated in ultralow attachment flasks (Corning Life Sciences, Amsterdam, The Netherlands) at 6×10^4 viable cells/mL in mammosphere medium, as previously described.³² Nonadherent spherical clusters of cells, named P1, were collected by gentle centrifugation after 7 days and disaggregated through enzymatic and mechanical dissociation. The cells were analyzed microscopically for single cellularity and seeded again at 6×10^4 viable cells/mL to generate nonadherent spherical clusters of cells, named P2.

RNA Isolation and RT-qPCR for mRNA and miRNA Detection

Total RNA was isolated from cells, mammospheres, and the II, III, and IV right mammary glands of mice bearing diffused atypical hyperplasia (6 weeks of age) and invasive lobular carcinomas (19 weeks of age) using the *mir*VanamiRNA isolation kit (Applied Biosystems, Milano, Italy). RNA was estimated qualitatively with an Agilent 2100 Bioanalyzer (Agilent Technologies, Cernusco sul Naviglio, Italy) and quantified with a NanoVuePlus Spectrophotometer (GE Healthcare, Milano, Italy). Total RNA was stored at -80°C until used. Quantitative PCRs (qPCRs) for miRNA detection were performed with TaqMan MicroRNA Assays (Applied Biosystems) on 10 ng total RNA, following manufacturer's instructions. For mRNA detection, 1 µg of DNase-treated RNA (DNA-free kit; Ambion, Austin, TX) was retrotranscribed with RETROscript reagents (Ambion), and qPCRs were performed using gene-specific primers (QuantiTect Primer Assay; Qiagen, Milano, Italy), SYBR Green (Applied Biosystems), and the 7900HT RT-PCR System (Applied Biosystems). Quantitative normalization was performed on the expression of sno-412, U6, or β -actin for miRNA or mRNA detection, respectively. The relative expression levels between samples were calculated using the comparative ΔC_T method.³⁵

EXIQON miRNA Expression Analysis

Two prototypic conditions were investigated using miRCURY-TM LNA Array, version 9.2 (EXIQON, San Francisco, CA), miRNA expression arrays: 19-week-old BALB-neuT animals (wk19.neu, three animals) and 10-week-old BALB-neuT animals (wk10.neu, four animals). Microarray data were generated by the EXIQON Profiling Service. The microarray experiment was based on a reference design, in which the reference is made of a pool of all samples under analysis. Background correction was done using the convolution model described by Ritchie et al³³ using an offset value of one. Intra-array Cy3/Cy5 normalization was done using the lowest method. Differentially expressed miRNAs were detected by regularized *t*-test using the oneChannelGUI Bioconductor package³⁴ (Supplemental Table S1).

qPCR Low-Density miRNA Arrays

Four conditions were investigated using Applied Biosystems Megaplex low-density qPCR miRNA expression arrays: 19-week-old BALB-neuT and BALB/c (wk19.neu and wk19.BALB/c, respectively) and 6-week-old BALB-neuT and BALB/c (wk6.neu and wk6.BALB/c, respectively) mice. Two animals were analyzed for each condition. qPCR runs were performed by technical support of Applied Biosystems. Raw C_T data were analyzed using Bioconductor.³⁶ Of 381 probes, 259 were left after removal of noninformative probes (those with a $C_T > 35$ in six of eight samples). ΔC_T values were calculated with respect to the mammalian U6 endogenous control (Supplemental Table S2). By using the rank product method,³⁷ differential expression was calculated between wk19.neu and wk19.BALB/c, between wk6.neu and wk6.BALB/c, and between wk19.neu and wk6.neu. This method addresses the multiple comparison problem and performs *P* value correction by false-discovery rate, comparing the true rank product distribution with a random one defined permuting miRNA labels in each of the cards under analysis. Herein, we have used 1000 permutations and a threshold of percentage of false-positive predictions of 0.05.

Massively Parallel Sequencing for miRNAs

Mammary glands from two wk19.BALB/c and two wk19.neu were evaluated. Total RNA (1.5 μ g) was used for SOLiD short RNA library preparation, following manufacturer's instructions (Applied Biosystems). Library preparation and sequence data generation were provided as service by Genomnia Srl (Milano, Italy). SOLiD, version 3, sequence data in color space, 35 color calls, were cleaned³⁸ and trimmed at 25 color calls to remove the P2 linker. Read mapping was done on the subset of ENSEMBL noncoding RNA (miRNA, rRNA, tRNA, small nucleolar RNA, and snRNA) using SHRIMP software version 1.3.2 (Toronto, ON, Canada)³⁹ with the following parameters: -n 1, -w 170%, -M miRNA, and -o 1. SHRIMP outputs were reformatted and imported into oneChannelGUI.³⁴ Differential expression analysis on count data was done using negative binomial dispersion⁴⁰ implemented in the edger Bioconductor package (threshold $P \leq 0.05$) (Supplemental Table S3).

miR-135b Meta-Analysis of Human Breast Cancers

The associations between miR-135a and miR-135b expression and survival and/or distant metastasis relapse were assessed using two data sets^{12,21} encompassing both miRNA and mRNA expression. For both of these data sets available on Gene Expression Omnibus (<http://www.ncbi.nlm.nih.gov/geo>; accession numbers GSE19536 and GSE22220), the expression data of miR-135a and miR-135b were extracted together with survival information. K-mean clustering ($k = 2$) was used to cluster samples in two groups: a set of samples characterized by the highest miR-135a and miR-135b average

expression level (high) and a set of samples characterized by the lowest miR-135a and miR-135b average expression level (low). A Cox proportional hazards regression model was fitted to survival data for high and low groups in the two data sets.

An Enerly et al¹² data set was also used to search for anti-correlation between miR-135b and its targets, MID1 and MTCH2. Samples were stratified on the basis of subgroups, as defined by Perou et al.⁴¹ Linear regression was used to measure and quantify anti-correlation between miR-135b and MID1 and MTCH2 expression data using Spearman's rank correlation test. Values between 0 and -1 indicate the presence of anti-correlation, whereas values between 0 and 1 indicate the presence of correlation.

Transient Cell Transfection

To obtain adherent TUBO or P1 derived cells silenced or overexpressing miR-135b, 3×10^5 or 1.2×10^5 cells per well in 6-well plates, respectively, were transfected using Lipofectamine 2000 (Invitrogen) with 200 nmol/L of miR-135b miRIDIAN Hairpin Inhibitor (anti-miR-135b antagomir) or 100 nmol/L of miR-135b miRIDIAN Mimics (miR-135b mimic) (Dharmacon; Thermo Fisher Scientific, Waltham, MA). For each experiment, cells were also transfected with miRIDIAN microRNA Hairpin Inhibitor (scrambled antagomir) or Mimics (scrambled mimic) negative controls. Cells were tested for miR-135b knockdown or overexpression 24, 48, and 72 hours after transfection.

To demonstrate a causal role of MID1 and MTCH2 downstream of miR-135b, a rescue experiment was performed by transfecting TUBO cells using Lipofectamine 2000 (Invitrogen) with 10 μ g of plasmids containing the cDNA of MID1 or MTCH2 genes without 3' untranslated region (UTR; Gene-Copoeia, Rockville, MD) and, thus, miR-135b insensitive. pVAX empty plasmid was used as a control. Forty-eight hours later, TUBO cells were transfected with 100 nmol/L of miR-135b miRIDIAN Mimics. Twenty-four hours later, 5×10^4 TUBO cells from each experimental condition were assayed in triplicate for their ability to grow in an anchorage-independent condition. At the same time, RNA was isolated from transfected cells to test miR-135b, MTCH2, and MID1 expression.

To obtain the phenocopy of miR-135b overexpression, knockdown of the MID1 target gene was obtained by transfecting 3×10^5 TUBO cells with 200 nmol/L of specific siRNA or nontargeting siRNA as control (ON-TARGET plus SMART pool siRNA; Dharmacon).

Flow Cytometry Analysis

TUBO, P1, P2, and P1 cells 24 hours after transfection were collected, disaggregated using enzymatic and mechanical dissociation, and washed in PBS supplemented with 0.2% bovine serum albumin and 0.01% sodium azide (Sigma-Aldrich). Cell suspensions were either stained for membrane

antigens or fixed and permeabilized with the Cytofix/Cytoperm Fixation/Permeabilization Kit (BD Biosciences, Milano, Italy) and then stained for intracellular antigens. The following antibodies were used: Alexa Fluor 647–conjugated anti-stem cell antigen (Sca)-1, allophycocyanin/Alexa Fluor 780–conjugated anti-Thy1.1 from Biologend (London, UK), and Alexa Fluor 647–conjugated anti-Nanog monoclonal antibody from eBioscience (Hatfield, UK). Samples were collected and analyzed using a CyAn ADP Flow Cytometer and Summit software version 4.3 (DakoCytomation, Heverlee, Belgium).

Sphere Generation Assay

TUBO cells were cultured at a density of 6×10^4 cells/mL in a 6-well, ultralow attachment plate in the mammosphere medium. After 5 days of culture, P1-derived cells were transfected with anti-miR-135b antagomir or scrambled antagomir. Five days after transfection, the total number of mammospheres for each well was counted and reported as number of mammospheres generated for every 10^3 cells plated.

Anchorage-Independent Growth Assays

Twenty-four hours after transfection, 5×10^4 TUBO cells were suspended in complete medium containing 0.45% Difco Noble Agar (BD Biosciences) and plated in 6-cm bacterial dishes. Medium was changed every 3 days. Fifteen days later, the dishes were stained with nitroblue tetrazolium (Sigma-Aldrich) and imaged with a Nikon SMZ1000 stereomicroscope. Colonies were counted with ImageJ software version 1.46 (NIH, Bethesda, MD).

Total Cell Count Assay

Twenty-four hours after transfection, TUBO cells were plated at 5×10^3 cells per well in 96-well plates in Dulbecco's modified Eagle's medium and starved for 24 hours. Complete medium was then added, and cells were allowed to grow for 1 to 4 days, fixed with 2.5% glutaraldehyde, and stained with 0.1% crystal violet. The dye was solubilized using 10% acetic acid. Optical density was measured with a Microplate Reader 680 XR (BioRad, Hercules, CA) at a 570-nm wavelength.

In Vivo Tumor Growth and Metastasis

Seven-week-old BALB/c female mice were challenged in the mammary pad with 1×10^5 TUBO cells. This pad was inspected weekly by palpation. Progressively growing masses >1 mm in diameter were regarded as tumors. Mice were sacrificed when one tumor exceeded a 10-mm mean diameter. For experimental metastasis assays, 2.5×10^4 TUBO, 5×10^4 TSA, or 4T1 cells were injected into the tail vein of 7-week-old female BALB/c mice. Mice were

sacrificed 20 days later, and total lungs were formalin fixed, cut into small pieces, paraffin embedded, divided into sections, and H&E stained. Micrometastases were evaluated, using an Olympus (Milano, Italy) BH2 microscope on three or more sections by using ImageJ software version 1.46.

miR-135b Target Identification

Detection of miR-135b targets was done by downloading from the Miranda database (<http://www.microrna.org>, last accessed September 1, 2010)⁴² all those characterized by an optimal or suboptimal miRSVR score,⁴² and retaining only those with a human orthologue (The Jackson Laboratory, Bar Harbor, ME; Mouse Genome Informatics Data and Statistical Reports, Mammalian Orthology: <ftp://ftp.informatics.jax.org/pub/reports/index.html#orthology>, last accessed September 1, 2010). The expression of these genes was then evaluated by transcriptome analysis (MOUSEREF-8 V2 Illumina bead chips, GSE28949, Illumina, San Diego, CA) in anti-miR-135b or scrambled transfected TUBO cells at 24, 48, and 72 hours after transfection. Each experimental condition was repeated three times. Complementary RNA synthesis and labeling were done with the Illumina RNA Amplification Kit (Ambion), following manufacturer's suggestions. Arrays were scanned on an Illumina BeadStation 500. Genome studio (Illumina) was used to generate a raw intensity signal without normalization. Data log₂ transformation and loess normalization were performed with oneChannelGUI.³⁴ After removal of unchanged and not expressed genes by interquartile range filtering⁴³ (only genes with an interquartile range >0.25 were retained), and linear model analysis⁴⁴ of differential expression, genes characterized by an uncorrected $P < 0.05$ and up-regulated in anti-miR-135b, compared with scrambled transfected TUBO cells, were considered for further analysis.

Luciferase Assay

A total of 3×10^5 TUBO cells were plated on a 6-well plate and, 24 hours later, cotransfected using Lipofectamine 2000 (Invitrogen) with 200 nmol/L of anti-miR-135b or 100 nmol/L of miR-135b mimic with 1 μg of pEZX-MT01 vector (Gene-Copoeia) containing the firefly luciferase gene, the 3' UTR of the indicated miR-135b potential target genes, and renilla luciferase as the tracking gene. Lysates were collected 72 and 96 hours after transfection, and firefly and renilla luciferase activities were measured with a dual Luciferase Reporter System (Promega, Madison, WI).

Protein Preparation and Immunoblotting

Total protein extracts were obtained from transfected TUBO cells by using a boiling buffer containing 0.125 mol/L Tris/HCl, pH 6.8, and 2.5% SDS. A protein-level evaluation of MID1 and MTCH2 was performed on total lysates collected 72 or 48 hours after transfection, respectively. Proteins (30 μg) were separated by SDS-PAGE and electroblotted

onto polyvinylidene fluoride membranes (BioRad, Milano, Italy). Membranes were blocked in 5% Blotto nonfat milk (Santa Cruz Biotechnology, Santa Cruz, CA) and Tris-buffered saline–Tween buffer [137 mmol/L NaCl, 20 mmol/L Tris/HCl (pH 7.6), and 0.1% Tween-20] for 1 hour at 37°C, then incubated with appropriate primary and secondary antibodies in 1% milk Tris-buffered saline–Tween buffer, overnight at 4°C and for 1 hour at room temperature, respectively, and visualized by enhanced chemiluminescence (Amersham Biosciences, Piscataway, NJ). The anti-MTCH2 rabbit polyclonal antibody was from ProteinTech (Chicago, IL); the anti-MID1 rabbit polyclonal antibody was from LSBio (Seattle, WA); and anti-actin mouse monoclonal, goat anti-mouse IgG horseradish peroxidase–conjugated, and goat anti-rabbit IgG horseradish peroxidase–conjugated antibodies were all from Santa Cruz Biotechnology. Protein modulations were calculated relative to controls, normalized on the actin loading control, and expressed as percentages by using Quantity One software version 4.6.3 (BioRad).

Results

Differential miRNA Expression in Invasive Carcinoma and in Normal Tissue during ErbB2 Mammary Carcinogenesis

To assess a correlation between deregulation of miRNAs and breast cancer, miRNA profiling was performed in BALB-neuT mice.^{24,28} Previous observations⁴⁵ showed that changes in the composition of mRNA species associated with modification of the cell composition of the mammary microenvironment can be used to tag tumor/microenvironment-associated genes. Herein, we used this approach to identify tumor-associated miRNAs. Two prototypic conditions of autochthonous carcinogenesis were investigated: diffused atypical hyperplasia present in the mammary glands of wk6.neu and invasive lobular carcinomas displayed by mammary glands of wk19.neu. Wild-type mammary glands from age-matched BALB/c animals (wk6.BALB/c and wk19.BALB/c) were included to account for miRNA changes as the result of physiological changes of the mammary glands. Transcription profiling was performed using real-time PCR low-density miRNA arrays. Principal component analysis shows that miRNA profile changes are mainly linked to animal age (Figure 1). However, some differences were observed between atypical hyperplasia and invasive carcinoma when they were compared with age-matched normal mammary tissue (Figure 1). Rank product statistics³⁷ did not disclose significant differences in miRNA expression of hyperplasia versus age-matched normal mammary tissue (wk6.neu versus wk6.BALB/c). In contrast, two tumor-associated miRNAs (mmu-miR-135a and mmu-miR-135b) were differentially expressed between lobular carcinoma and age-matched normal mammary tissue (wk19.neu versus wk19.BALB/c). Their expression was confirmed in the mammary glands of 19-week-old BALB/c and BALB-neuT mice by qPCR on independent samples. No differences in the expression level were observed

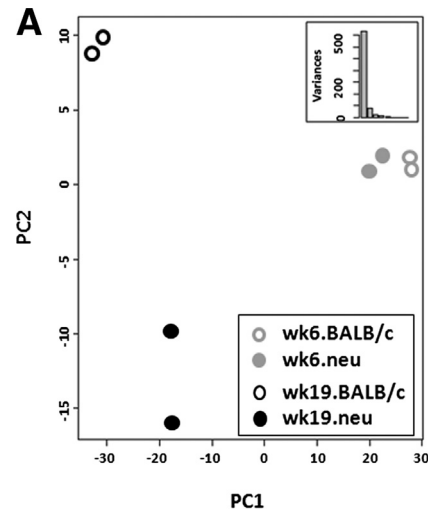


Figure 1 Principal component analysis of global miRNA expression changes. Transcription profiling of mammary gland samples from 6-week-old BALB-neuT (wk6.neu), 19-week old BALB-neuT (wk19.neu), and age-matched wild-type BALB/c (wk6.BALB/c and wk19.BALB/c) mice was performed using Applied Biosystems real-time PCR low-density miRNA arrays. miRNA expression profile changes are mainly linked to animal age; however, that of invasive carcinoma is different from that of age-matched normal mammary tissue (black closed versus white open circles), whereas that of atypical hyperplasia and normal tissue is more similar (gray closed versus white open circles). Amount of variance explained by each of the principal component analysis components is shown in the inset.

comparing wk6.BALB/c with wk6.neu for both miR-135a and miR-135b, whereas a statistically significant increase was observed comparing wk19.BALB/c with wk19.neu (Figure 2). Furthermore, although miR-135a and miR-135b expression levels were comparable between wk6.BALB/c and wk19.BALB/c, a statistically significant expression increment was found comparing wk6.neu with wk19.neu (Figure 2, A and B), suggesting a correlation between miRNA expression and tumor mass increase. Massively parallel sequencing of RNA, or RNA-seq, quantitative analysis performed on independent samples displayed a statistically significant increment only for miR-135a and miR-135b in wk19.neu compared with that measured in wk19.BALB/c (miR-135a log₂ fold change, 3.19 false-discovery rate <0.05; miR-135b log₂ fold change, 4.36 false-discovery rate <0.05). RNA-seq data were also used to evaluate miR-135a and miR-135b absolute concentrations. Their ranking in wk19.BALB/c and in wk19.neu showed that they move from the bulk of low-expressed miRNAs (>200 miRNAs) to a subgroup with medium expression (approximately 60 miRNAs) (Supplemental Figure S1).

miR-135a and miR-135b in Human Cancers

Little is known about the association of miR-135a and miR-135b with human breast cancer.^{13,14} However, Blenkiron et al¹⁰ data set performed on 93 primary human breast tumors highlighted that miR-135b is up-regulated in basal and normal-like breast cancer subgroups.⁴¹ Moreover, Enerly et al¹² data set

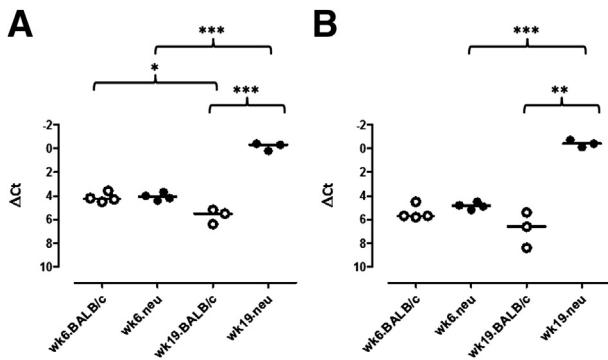


Figure 2 miR-135a (A) and miR-135b (B) expression levels measured in the mammary glands of 6- and 19-week-old BALB/c (white open circles) and BALB-neuT (black closed circles) mice measured by qPCR. Each dot represents the evaluation of miRNA levels in a single mouse. ΔC_T values were calculated with respect to the mammalian sno-412 RNA level. Statistically significant differences were calculated using the Student's *t*-test: wk6.BALB/c versus wk19.BALB/c ($*P = 0.01$) for miR-135a, wk6.neu versus wk19.neu ($***P < 0.0001$) for miR-135a and miR-135b, and wk19.BALB/c versus wk19.neu ($**P < 0.001$ for miR-135b and $***P < 0.0001$ for miR-135a).

on 101 primary human breast tumors confirmed the overexpression of miR-135b in basal-like tumor subtypes. Genome-wide investigations of miRNA status in primary human breast cancers done by Enerly¹² and Buffa²¹ and coworkers are valuable tools to investigate the association between miRNA expression and patient survival or distant metastasis relapse, respectively. By using these data and applying a Cox proportional hazards regression model, a statistical association between miR-135b up-modulation and poor survival ($P = 0.04$) was observed (Supplemental Figure S2A); however, no correlation with late (ie, 120 months) distant metastasis was revealed (Supplemental Figure S2B). Nevertheless, up-modulation of miR-135b seems to be involved in early (ie, 50 months) distant metastasis relapse (Supplemental Figure S2C). miR-135a expression does not show any significant association with patient survival and distant metastasis appearance (data not shown).

miR-135b Does Not Affect *in Vitro* or *in Vivo* BALB-neuT Tumor Cell Line Proliferation

The overexpression of miR-135b in invasive mammary tumors of BALB-neuT mice, together with its correlation with poor survival in patients with breast cancer, prompted us to explore its role in tumor cell proliferation. qPCR performed on three cell lines derived from BALB-neuT mammary tumors and on two other unrelated BALB/c mammary tumor cell lines (TSA³¹ and 4T1) showed that miR-135b was expressed in all tested cell lines, even if at a lower level in both TSA and 4T1 cells compared with BALB-neuT tumor cells (Supplemental Figure S3). The consequences of miR-135b deregulation were investigated in BALB-neuT line 1 (TUBO), TSA, and 4T1 cells. qPCR analysis 72 hours after transfection showed that miR-135b expression was almost completely abrogated when TUBO, TSA, and 4T1 cells were transfected with specific antisense

inhibitors (anti-miR-135b) and strongly up-regulated after its transient overexpression by specific mimics (miR-135b-over) (data not shown). By contrast, miR-135b expression was not affected after transfection with negative controls (scrambled). Both down-regulation and overexpression of miR-135b had a marginal effect on TUBO total cell count (Figure 3): only a 10% to 15% reduction of total cell number was observed in anti-miR-135b compared with scrambled TUBO cells (Figure 3A) and 5% to 20% enhancement of total cell number in miR-135b-over compared with scrambled TUBO cells (Figure 3B). Comparable results were observed when miR-135b deregulation was studied on both TSA and 4T1 cells (data not shown). When TUBO cells in which miR-135b was silenced or overexpressed were injected s.c. in the flank of BALB/c mice, only a marginal effect on tumor incidence was observed (Figure 3, C and D), although tumor growth speed was not affected at all (data not shown).

miR-135b Is Involved in CSC Self-Renewal

Because miRNAs are involved in CSC phenotype maintenance by connecting stemness and metastasis,⁸ an *in vitro* cultivation system that allows propagation of mammary epithelial TUBO cells in suspension as nonadherent mammospheres³² was used to assess the miR-135b level of expression in TUBO cell-derived nonadherent mammospheres and in differentiated mammary TUBO cells.

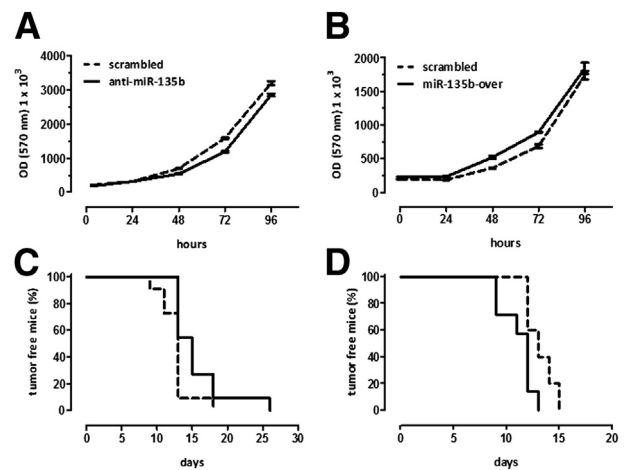


Figure 3 miR-135b expression does not significantly affect tumor cell growth both *in vitro* and *in vivo*. TUBO cells were transfected with a specific miR-135b antisense inhibitor (anti-miR-135b) or mimic (miR-135b-over) or their negative controls (scrambled). A and B: TUBO cell proliferation was evaluated 24, 48, 72, and 96 hours after down-regulation (A) or overexpression (B) of miR-135b. Three independent experiments (at least in quadruplicate) were performed, and a representative one is shown as means \pm SEM. C and D: The miR-135b effect on TUBO cell growth *in vivo* was evaluated after injecting s.c. into BALB/c mice anti-miR-135b (C; continuous black line, $n = 11$) or miR-135b-over (D; continuous black line, $n = 7$). In each experiment, TUBO cells were also transfected with negative scrambled anti-miR (C; dotted black line, $n = 11$) and a scrambled mimic (D; dotted black line, $n = 5$). Data are expressed as tumor incidence; differences were analyzed by the log-rank (Mantel-Cox) test.

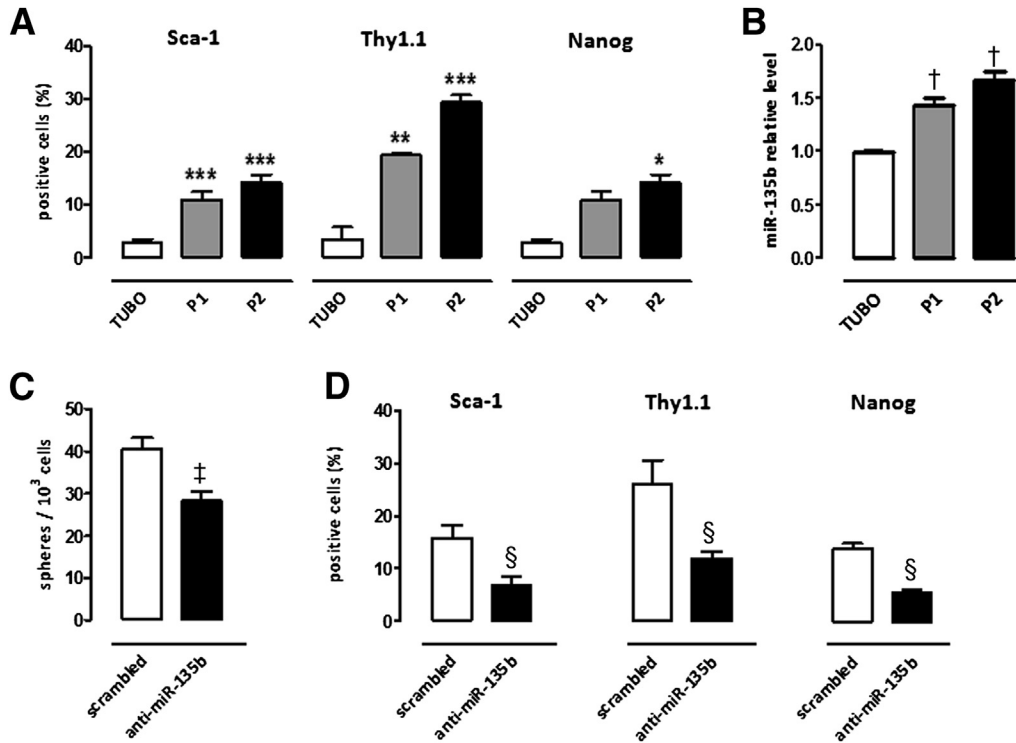


Figure 4 miR-135b expression is significantly higher in mammospheres compared with differentiated epithelial TUBO cells and is involved in CSC self-renewal. **A:** Fluorescence-activated cell sorter (FACS) analysis of Sca-1, Thy1.1, and Nanog stem cell markers on TUBO, P1, and P2 mammospheres. Data are expressed as means ± SEM of the percentage of positive cells. A two-tailed Student's *t*-test was used for comparisons between P1 or P2 mammospheres and TUBO cells. **P* = 0.02, ***P* = 0.002, and ****P* = 0.0009. **B:** miR-135b level in P1 and P2, measured by qPCR and expressed as 2^{-ΔΔC} normalized to TUBO cells grown in mammosphere medium. A two-tailed Student's *t*-test was used for comparisons. †*P* = 0.003. **C:** Sphere generation assay 5 days after transfection of P1-derived cells with anti-miR-135b or scrambled antagonist. Data are expressed as mammosphere number per 10³ plated cells. A two-tailed Student's *t*-test was used for comparisons. ‡*P* = 0.01. **D:** FACS analysis of Sca-1, Thy1.1, and Nanog stem cell markers on P1-derived cells 24 hours after transfection with anti-miR-135b or scrambled antagonist. Data are expressed as means ± SEM of the percentage of positive cells. A two-tailed Student's *t*-test was used for comparisons between scrambled and miR-135b antagonist-transfected P1-derived cells. §*P* = 0.004.

Fluorescence-activated cell sorter analysis of some stem cell markers showed that the percentage of Sca-1,³² Thy1.1,⁴⁶ and Nanog⁴⁷ positive cells significantly increased progressively from TUBO to P1 and P2 passages of mammospheres (Figure 4A). The level of miR-135b was significantly higher in P1 and P2 mammospheres compared with that of differentiated TUBO cells (Figure 4B). Similar results were observed when miR-135b expression was assessed in mammospheres from TSA (Supplemental Figure S4). To further analyze miR-135b involvement in CSC self-renewal, P1 mammospheres were transfected with anti-miR-135b or scrambled antagonist, and sphere generation was evaluated. As reported in Figure 4C, miR-135b silencing significantly reduced mammosphere generation in a sphere generation assay. This inhibition was associated with a reduction in the percentage of Sca-1-, Thy1.1-, and Nanog-expressing cells (Figure 4D).

miR-135b Overexpression Enhances Colony Formation *in Vitro* and Metastasis Formation *in Vivo*

Eneryl¹² and Buffa²¹ and coworkers' meta-analyses suggest a correlation between miR-135b overexpression in breast

cancer and poor survival and early metastasis relapse. We, thus, looked to see whether miR-135b has any activity linked to metastasis formation in BALB-neuT mammary cancer cells. Anchorage-independent growth in soft agar was evaluated by both silencing and overexpressing miR-135b in TUBO cells. Anti-miR-135b TUBO cells cultured in soft agar showed a significant reduction in the number of colonies compared with those observed with scrambled TUBO cells (98.3 ± 14.4 versus 203.0 ± 9.5 colonies; *P* = 0.004) (Figure 5A), whereas a significant enhancement of the number of colonies was observed in miR-135b-over compared with scrambled TUBO cells (148.7 ± 12.1 versus 96.5 ± 10.4 colonies; *P* = 0.02) (Figure 5B). Because of its ability to enhance anchorage-independent growth, we also investigated whether miR-135b influences metastasis formation *in vivo*. Thus, anti-miR-135b or miR-135b-over TUBO cells were injected into the tail vein of BALB/c mice, and lung micrometastases were counted. Anti-miR-135b TUBO cells were significantly (*P* = 0.02) less able to seed and formed fewer lung metastases than the scrambled TUBO cells (Figure 5C). In contrast, significantly (*P* = 0.01) more lung metastases were observed for miR-135b-over when compared with scrambled TUBO cells (Figure 5D). Up-regulation of

miR-135b in both TSA and 4T1 cells resulted in an increase of the number of lung metastases when injected in BALB/c mice, suggesting a role of miR-135b in tumor metastatization in these tumor cell lines (Supplemental Figure S5).

miR-135b Target Genes

The first step in the detection of miR-135b targets was the extraction of all predicted mouse miR-135b targets (3888 genes) from the Miranda database (<http://www.microrna.org>, last accessed September 1, 2012),⁴² retaining only those having a human orthologue (1054 genes). The following step was to evaluate their differential expression in anti-miR-135b or in scrambled TUBO cells 72 hours after transfection by Illumina microarrays. More important, qPCR data showed that miR-135b expression reached nearly 100% of reduction only at 72 hours (Supplemental Figure S6). The 17 genes up-regulated in anti-miR-135b TUBO cells were considered as putative miR-135b targets (Table 1). Because down-regulation of two of them only (MID1 and MTCH2) was known to be associated with a more aggressive phenotype in solid tumors,^{48,49} we focused our attention on them.

To determine whether MID1 and MTCH2 are bona fide targets of miR-135b, two reporter vectors with MID1 and MTCH2 3' UTR fragments containing the miR-135b binding sequences (Supplemental Figure S7) were used to perform luciferase assays. As shown in Figure 6A, luciferase expression driven by the 3' UTRs of MID1 and MTCH2 was significantly enhanced in anti-miR-135b compared with scrambled TUBO cells. Consistent with the luciferase and the genome-wide microarray analysis results, MID1 and MTCH2 mRNA levels, measured by qPCR, were significantly enhanced in anti-miR-135b TUBO cells compared with those in scrambled TUBO cells (Figure 6B). Modulation of MID1 and MTCH2 mRNAs corresponded to fluctuations of MID1 and MTCH2 protein levels (10% and 20%, respectively) in anti-miR-135b compared with those measured in scrambled TUBO cells (Figure 6C). Moreover, miR-135b overexpression in TUBO cells was associated with a decrease of MID1 and MTCH2 protein levels (−93% and −23%, respectively) (Figure 6C). We then investigated the possible direct regulation of MID1 and MTCH2 by miR-135b *in vivo*, by comparing their mRNA expression during BALB-neuT mammary tumor progression. A significant reduction in mRNA of MID1 and MTCH2 was observed in wk19.neu versus wk6.neu mammary glands (Figure 6D).

To evaluate whether the prometastatic effect mediated by miR-135b is MID1 or MTCH2 dependent, we measured the anchorage-independent colony formation ability of miR-135b overexpressing TUBO cells also expressing MID1 or MTCH2 coding sequences lacking the 3' UTR; therefore, they yielded a product resistant to miR-135b-mediated suppression. miR-135b mimic-transfected TUBO cells overexpressing MID1 or MTCH2 miR-135b-insensitive cDNA showed a significant reduction of colony formation ability compared with that measured in miR-135b mimic TUBO

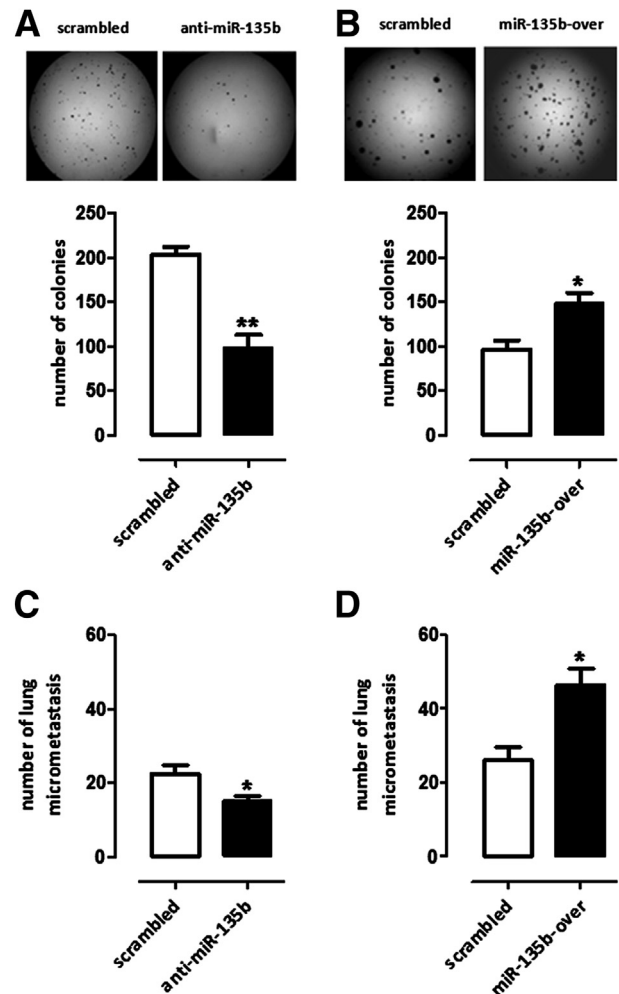


Figure 5 miR-135b expression significantly enhances anchorage-independent growth *in vitro* and metastasis formation *in vivo*. TUBO cells were transfected with specific anti-miR-135b (A and C: black bars) or miR-135b mimic (B and D: black bars) or their scrambled controls (white bars). A and B: TUBO cell ability to grow in soft agar and form colonies was evaluated 15 days after down-regulation (A) or overexpression (B) of miR-135b. Three independent experiments were performed in triplicate, and a representative one is shown. Results are shown as means \pm SEM of one of three independent experiments. A two-tailed Student's *t*-test was used for comparisons. **P* = 0.02; ***P* = 0.004. C and D: Lung micrometastasis formation was evaluated 20 days after tail vein injection of transfected TUBO cells in BALB/c mice (*n* = 4 to 5 mice for each group) on H&E-stained total lung sections. Results are shown as means \pm SEM of one out of three independent experiments performed in triplicates. A two-tailed Student's *t*-test was used for comparisons. **P* = 0.02.

cells also transfected with the empty plasmid (Figure 7). In addition, to further confirm the direct link between MID1 and colony formation ability of TUBO cells, a phenocopy experiment of miR-135b overexpression was performed by silencing the *MID1* target gene with specific siRNA. Significantly more colonies were observed after MID1 knockdown (Supplemental Figure S8). Taken together, these data indicate that the down-regulation of MID1 and MTCH2 by miR-135b is the mechanism by which miR-135b promotes anchorage-independent progression of ErbB2-driven mammary carcinomas.

Table 1 miR-135b Putative Targets

Probe ID	Entrez ID	Gene symbol	Log ₂ FC variation	Log ₂ average fluorescence intensity	P value
ILMN_1238032	242960	<i>FBXL5</i>	0.73	9.87	0.001
ILMN_1244768	20818	<i>SRPRB</i>	1.12	10.35	0.002
ILMN_2619452	17318	<i>MID1</i>	0.54	8.38	0.003
ILMN_2718612	68291	<i>MTO1</i>	0.56	9.37	0.004
ILMN_2654568	72133	<i>TRUB1</i>	0.71	9.13	0.007
ILMN_2914271	11836	<i>ARAF</i>	0.82	11.32	0.010
ILMN_2755981	226151	<i>FAM178A</i>	0.97	10.11	0.011
ILMN_2610204	56428	<i>MTCH2</i>	0.64	9.52	0.011
ILMN_2710705	18412	<i>SQSTM1</i>	0.89	12.36	0.015
ILMN_2668387	106143	<i>CGGBP1</i>	0.59	11.39	0.020
ILMN_2737296	102436	<i>LARS2</i>	0.41	9.28	0.022
ILMN_1229418	12807	<i>HPS3</i>	0.56	8.99	0.022
ILMN_1226187	14768	<i>LANCL1</i>	0.72	9.82	0.023
ILMN_3009880	242700	<i>IL28RA</i>	0.36	8.78	0.024
ILMN_1258977	67878	<i>TMEM33</i>	0.78	11.28	0.039
ILMN_1225723	72085	<i>OSGEPL1</i>	0.45	9.36	0.042
ILMN_2757150	18555	<i>PCTK1</i>	0.50	10.01	0.047

The 17 genes in the table were obtained by the intersection of genes detected as up-regulated on miR-135b silencing ($P \leq 0.05$) and the putative target of miR-135b extracted from the Miranda database.

FC, fold change.

Taking advantage of the available data on miRNA status and mRNA transcription profile, published by Enerly et al,¹² we looked for the presence of an anti-correlation between miR-135b expression and MID1 or MTCH2 modulation in primary human breast cancers. Because miR-135b is significantly up-modulated only in basal and normal-like breast cancer subtypes, as shown by Blenkinsop et al,¹⁰ we stratified the mRNA data on the basis of the clinical annotation available for the Enerly et al¹² data set. A clear anti-correlation between miR-135b and MID1 and MTCH2 was found in the subset of tumors defined as normal-like (Supplemental Figure S9), reinforcing the relevance of miR-135b and its targets in breast tumorigenesis.

Discussion

During the past 10 years, miRNAs have attracted attention because of their ability to post-transcriptionally modulate the expression of oncogenes and oncosuppressors. Several reports have described their involvement in the initiation and progression of most cancers. miRNAs overexpressed in tumors contribute to oncogenesis by deregulating tumor suppressors, whereas miRNAs lost by tumors participate in oncogene overexpression. Notably, roles of miRNAs in cancer are tissue and tumor specific, and alterations in miRNA expression alone can cause cell neoplastic transformation.⁵⁰ In addition, a specialized family of miRNAs (metastamir) modulates the metastatic behavior of neoplastic cells⁵¹ and is involved in the regulation of the epithelial-mesenchymal transition.⁵² miRNAs may also contribute to the metastatic program by both modulating the structure of local tumor microenvironment and promoting neoangiogenesis during tumor progression.⁵³

The mutated form of the rat ErbB2 oncogene drives aggressive mammary carcinogenesis in BALB-neuT mice. The steps of this progression, mimicking a few features of human breast tumors,²³ have been extensively characterized at the transcriptional level.^{54–56} The analysis of miRNA expression reported herein shows increased expression of miR-135a and miR-135b during tumor expansion in function of the mouse age. The decreased expression of these two miRNAs observed in function of the age in the mammary glands of normal mice endorses their involvement in tumor development.

Little is known about the expression of these two miRNAs in tumors. miR-135a down-regulation has been associated with the anti-cancer effect of mistletoe lectin-I⁵⁷ and with a higher probability of relapse in patients with classic Hodgkin lymphoma.⁵⁸ Recently, miR-135a and miR-135b up-modulation has been shown to correlate with the degree of malignancy in colon cancer,^{59–61} osteosarcoma,⁶² ependymoma,⁶³ and hepatocellular carcinoma.⁶⁴ Although miR-135a and miR-135b involvement in breast cancer has never been described, by exploiting data on the expression of miRNAs in human breast cancers,^{12,21} the overexpression of miR-135b, but not miR-135a, appeared to be associated with poor prognosis. In addition, miR-135b overexpression in basal-like and estrogen-negative human tumors, shown by this meta-analysis, fits in well with the notion that mammary tumors of BALB-neuT mice are similar to basal-like and estrogen-negative human mammary carcinomas.²⁶

TUBO cells were established from a BALB-neuT mammary carcinoma.⁶⁵ As expected, because TUBO cells are ErbB2 addicted, miR-135b expression was not strictly involved in promoting their proliferation, neither *in vitro* nor *in vivo*, but was associated with their anchorage-independent growth and

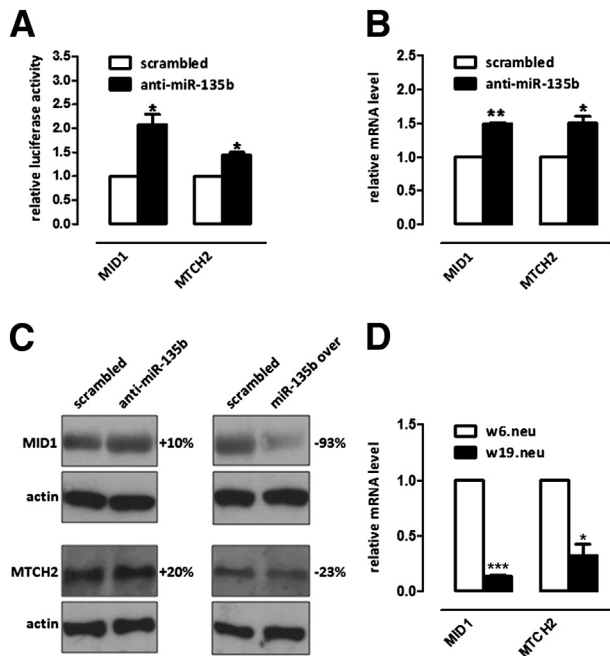


Figure 6 miR-135b down-regulates MID1 and MTCH2 target genes. **A:** Luciferase assays performed on TUBO cells cotransfected with reporter constructs containing the 3' UTR of the indicated genes cloned downstream of the luciferase coding sequence, together with anti-miR-135b or scrambled anti-miR. Results were calculated as fold changes and are shown as means \pm SEM of firefly luciferase activity relative to controls, normalized on renilla luciferase activity. A two-tailed Student's *t*-test was used for comparisons. $*P = 0.03$. Three independent experiments were performed in triplicate, and a representative one is shown. **B:** MID1 and MTCH2 mRNA levels measured by qPCR in TUBO cells 72 hours after anti-miR-135b or scrambled anti-miR transfection. Results were calculated as fold changes (means \pm SEM) relative to scrambled, normalized on β -actin. A two-tailed Student's *t*-test was used for comparisons. $*P = 0.03$, $**P = 0.001$. **C:** MID1 and MTCH2 protein levels measured by using Western blot analysis in TUBO cells transfected with anti-miR-135b (left panels), miR-135b mimic (right panels), or their scrambled controls. The percentage indicated on the right refers to protein modulations. **D:** MID1 and MTCH2 mRNA levels measured by qPCR in the mammary tissue from 6-week-old (wk6.neu, white bars) and 19-week-old (wk19.neu, black bars) BALB-neuT mice. Results were calculated as fold changes (means \pm SEM) relative to wk6.neu, normalized on β -actin. For all data, a two-tailed Student's *t*-test was used for comparisons. $*P = 0.02$, $***P = 0.0002$.

their ability to produce lung metastasis. Moreover, expression of miR-135b increases in nonadherent spherical clusters of different breast cancer cell lines that display increased tumorigenic and metastatic ability.³² Furthermore, miR-135b involvement in CSC phenotype maintenance is demonstrated by the significant reduction of mammospheres after its silencing in P1-derived TUBO cells.

To investigate the molecular mechanism underlying miR-135b functionality, we searched for its targets by computational prediction. However, the specificity and sensitivity of the existing algorithms are still too poor to generate meaningful, workable hypotheses for subsequent experimental testing.⁶⁶ Integration of prediction with other experimental methods investigating target modulation is, thus, required to improve target detection specificity. Although miRNAs only

partially suppress gene expression and promote mRNA decay, a certain effect at the level of target mRNA concentration can be detected with carefully designed microarray experiments.⁶⁷ Combining target prediction knowledge derived from Miranda with a gene expression profile experiment, in which we look for up-regulated genes after miR-135b silencing in TUBO cells, we detected 17 putative targets. However, among all these genes, only *MID1* and *MTCH2* expression was associated with a statistically significant up-regulation 72 hours after miR-135b silencing in TUBO cells, suggesting a direct link to this miRNA. Moreover, *MID1* and *MTCH2* down-modulation in tumor cells has been reported to be associated with a more aggressive phenotype, which is part of a gene signature associated with metastasis and survival in solid tumors.^{48,49} *MID1* forms homodimers that associate with microtubules in the cytoplasm, and is probably involved in the formation of multiprotein structures acting as anchor points for microtubules.⁶⁸ *MTCH2*, also called Met-induced mitochondrial protein,⁶⁹ is an outer mitochondrial membrane protein whose induction causes growth and motility arrest *in vitro* and loss of tumorigenicity *in vivo*⁶⁹ and facilitates apoptosis.⁷⁰ The luciferase assay showed that both are bona fide miR-135b targets. The role of miR-135b in anchorage-independent cell growth and the fact that *MID1* and *MTCH2* down-regulation is associated with increased invasiveness in both BALB-neuT mice and in solid human cancers^{48,49} indicate a role of miR-135b in invasion and metastasis formation in breast cancer. Moreover, the presence of an anti-correlation between miR-135b and *MID1* and *MTCH2* expressions in human breast cancer specimens of normal-like subtype

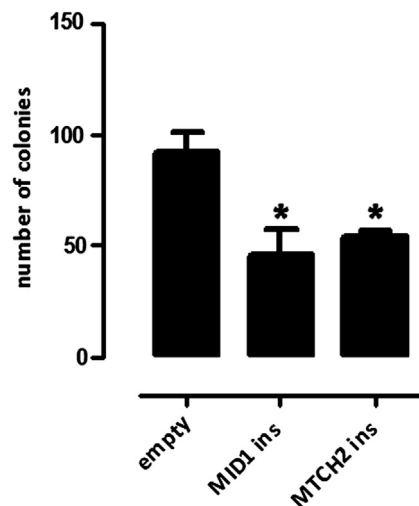


Figure 7 miR-135b prometastatic effect is mediated by *MID1* and *MTCH2*. Number of soft agar colonies generated from TUBO cells transfected with miR-135b-insensitive *MID1* (*MID1 ins*), *MTCH2* (*MTCH2 ins*), or the empty vector (as control) and then with miR-135b mimic. Three independent experiments were performed in triplicate, and a representative one is shown. A two-tailed Student's *t*-test was used to compare each experimental condition with that of miR-135b-overexpressing TUBO cells transfected also with empty plasmid. $*P = 0.04$.

highlighted the relevance of the whole study for the understanding of human breast cancer.

The detection of the role of miR-135b in BALB-neuT mammary carcinogenesis provides a well-characterized pre-clinical model for exploration of the potentiality of miR-135b, MID1, and MTCH2 as new therapeutic targets.

Supplemental Data

Supplemental material for this article can be found at <http://dx.doi.org/10.1016/j.ajpath.2013.02.046>.

References

- Jemal A, Siegel R, Xu J, Ward E: Cancer statistics, 2010. *CA Cancer J Clin* 2010, 60:277–300
- Galvao ER, Martins LM, Ibiapina JO, Andrade HM, Monte SJ: Breast cancer proteomics: a review for clinicians. *J Cancer Res Clin Oncol* 2011, 137:915–925
- Gupta GP, Massague J: Cancer metastasis: building a framework. *Cell* 2006, 127:679–695
- Nguyen DX, Bos PD, Massague J: Metastasis: from dissemination to organ-specific colonization. *Nat Rev Cancer* 2009, 9:274–284
- Valastyan S, Weinberg RA: Tumor metastasis: molecular insights and evolving paradigms. *Cell* 2011, 147:275–292
- Nair VS, Maeda LS, Ioannidis JP: Clinical outcome prediction by microRNAs in human cancer: a systematic review. *J Natl Cancer Inst* 2012, 104:528–540
- Tavazoie SF, Alarcon C, Oskarsson T, Padua D, Wang Q, Bos PD, Gerald WL, Massague J: Endogenous human microRNAs that suppress breast cancer metastasis. *Nature* 2008, 451:147–152
- Zhang J, Ma L: MicroRNA control of epithelial-mesenchymal transition and metastasis. *Cancer Metastasis Rev* 2012, 31:653–662
- Bockmeyer CL, Christgen M, Muller M, Fischer S, Ahrens P, Langer F, Kreipe H, Lehmann U: MicroRNA profiles of healthy basal and luminal mammary epithelial cells are distinct and reflected in different breast cancer subtypes. *Breast Cancer Res Treat* 2011, 130:735–745
- Blenkiron C, Goldstein LD, Thorne NP, Spiteri I, Chin SF, Dunning MJ, Barbosa-Morais NL, Teschendorff AE, Green AR, Ellis IO, Tavare S, Caldas C, Miska EA: MicroRNA expression profiling of human breast cancer identifies new markers of tumor subtype. *Genome Biol* 2007, 8:R214
- Adams BD, Guttilla IK, White BA: Involvement of microRNAs in breast cancer. *Semin Reprod Med* 2008, 26:522–536
- Enerly E, Steinfeld I, Kleivi K, Leivonen SK, Aure MR, Russnes HG, Ronneberg JA, Johnsen H, Navon R, Rodland E, Makela R, Naume B, Perala M, Kallioniemi O, Kristensen VN, Yakhini Z, Borresen-Dale AL: miRNA-mRNA integrated analysis reveals roles for miRNAs in primary breast tumors. *PLoS One* 2011, 6:e16915
- Lowery AJ, Miller N, Devaney A, McNeill RE, Davoren PA, Lemetre C, Benes V, Schmidt S, Blake J, Ball G, Kerin MJ: MicroRNA signatures predict oestrogen receptor, progesterone receptor and HER2/neu receptor status in breast cancer. *Breast Cancer Res* 2009, 11:R27
- Iorio MV, Ferracin M, Liu CG, Veronese A, Spizzo R, Sabbioni S, Magri E, Pedriali M, Fabbri M, Campiglio M, Menard S, Palazzo JP, Rosenberg A, Musiani P, Volinia S, Nenci I, Calin GA, Querzoli P, Negrini M, Croce CM: MicroRNA gene expression deregulation in human breast cancer. *Cancer Res* 2005, 65:7065–7070
- Sachdeva M, Mo YY: MicroRNA-145 suppresses cell invasion and metastasis by directly targeting mucin 1. *Cancer Res* 2010, 70:378–387
- Png KJ, Yoshida M, Zhang XH, Shu W, Lee H, Rimmer A, Chan TA, Comen E, Andrade VP, Kim SW, King TA, Hudis CA, Norton L, Hicks J, Massague J, Tavazoie SF: MicroRNA-335 inhibits tumor reinitiation and is silenced through genetic and epigenetic mechanisms in human breast cancer. *Genes Dev* 2011, 25:226–231
- Zhu N, Zhang D, Xie H, Zhou Z, Chen H, Hu T, Bai Y, Shen Y, Yuan W, Jing Q, Qin Y: Endothelial-specific intron-derived miR-126 is down-regulated in human breast cancer and targets both VEGFA and PIK3R2. *Mol Cell Biochem* 2011, 351:157–164
- Ma L: Role of miR-10b in breast cancer metastasis. *Breast Cancer Res* 2010, 12:210
- Song B, Wang C, Liu J, Wang X, Lv L, Wei L, Xie L, Zheng Y, Song X: MicroRNA-21 regulates breast cancer invasion partly by targeting tissue inhibitor of metalloproteinase 3 expression. *J Exp Clin Cancer Res* 2010, 29:29
- Rothe F, Ignatiadis M, Chaboteaux C, Haibe-Kains B, Kheddoumi N, Majaj S, Badran B, Fayyad-Kazan H, Desmedt C, Harris AL, Piccart M, Sotiriou C: Global microRNA expression profiling identifies MiR-210 associated with tumor proliferation, invasion and poor clinical outcome in breast cancer. *PLoS One* 2011, 6:e20980
- Buffa FM, Camps C, Winchester L, Snell CE, Gee HE, Sheldon H, Taylor M, Harris AL, Ragoussis J: microRNA-associated progression pathways and potential therapeutic targets identified by integrated mRNA and microRNA expression profiling in breast cancer. *Cancer Res* 2011, 71:5635–5645
- Andorfer CA, Necela BM, Thompson EA, Perez EA: MicroRNA signatures: clinical biomarkers for the diagnosis and treatment of breast cancer. *Trends Mol Med* 2011, 17:313–319
- Cavallo F, Offringa R, van der Burg SH, Forni G, Melief CJ: Vaccination for treatment and prevention of cancer in animal models. *Adv Immunol* 2006, 90:175–213
- Quaglino E, Mastini C, Forni G, Cavallo F: ErbB2 transgenic mice: a tool for investigation of the immune prevention and treatment of mammary carcinomas. *Curr Protoc Immunol* 2008, Chap 20:Unit 20.9.1–20.9–10
- Husemann Y, Geigl JB, Schubert F, Musiani P, Meyer M, Burghart E, Forni G, Eils R, Fehm T, Riethmuller G, Klein CA: Systemic spread is an early step in breast cancer. *Cancer Cell* 2008, 13:58–68
- Astolfi A, Landuzzi L, Nicoletti G, De Giovanni C, Croci S, Palladini A, Ferrini S, Iezzi M, Musiani P, Cavallo F, Forni G, Nanni P, Lollini PL: Gene expression analysis of immune-mediated arrest of tumorigenesis in a transgenic mouse model of HER-2/neu-positive basal-like mammary carcinoma. *Am J Pathol* 2005, 166:1205–1216
- Quaglino E, Rolla S, Iezzi M, Spadaro M, Musiani P, De Giovanni C, Lollini PL, Lanzardo S, Forni G, Sanges R, Crispi S, De Luca P, Calogero R, Cavallo F: Concordant morphologic and gene expression data show that a vaccine halts HER-2/neu preneoplastic lesions. *J Clin Invest* 2004, 113:709–717
- Boggio K, Nicoletti G, Di Carlo E, Cavallo F, Landuzzi L, Melani C, Giovarelli M, Rossi I, Nanni P, De Giovanni C, Bouchard P, Wolf S, Modesti A, Musiani P, Lollini PL, Colombo MP, Forni G: Interleukin 12-mediated prevention of spontaneous mammary adenocarcinomas in two lines of Her-2/neu transgenic mice. *J Exp Med* 1998, 188:589–596
- Workman P, Aboagye EO, Balkwill F, Balmain A, Bruder G, Chaplin DJ, Double JA, Everitt J, Farningham DA, Glennie MJ, Kelland LR, Robinson V, Stratford IJ, Tozer GM, Watson S, Wedge SR, Eccles SA: Guidelines for the welfare and use of animals in cancer research. *Br J Cancer* 2010, 102:1555–1577
- Rovero S, Boggio K, Di Carlo E, Amici A, Quaglino E, Porcedda P, Musiani P, Forni G: Insertion of the DNA for the 163-171 peptide of IL1beta enables a DNA vaccine encoding p185(neu) to inhibit mammary carcinogenesis in Her-2/neu transgenic BALB/c mice. *Gene Ther* 2001, 8:447–452

31. Nanni P, de Giovanni C, Lollini PL, Nicoletti G, Prodi G: TS/A: a new metastasizing cell line from a BALB/c spontaneous mammary adenocarcinoma. *Clin Exp Metastasis* 1983, 1:373–380
32. Grange C, Lanzardo S, Cavallo F, Camussi G, Bussolati B: Sca-1 identifies the tumor-initiating cells in mammary tumors of BALB-neuT transgenic mice. *Neoplasia* 2008, 10:1433–1443
33. Ritchie ME, Silver J, Oshlack A, Holmes M, Diyagama D, Holloway A, Smyth GK: A comparison of background correction methods for two-colour microarrays. *Bioinformatics* 2007, 23:2700–2707
34. Sanges R, Cordero F, Calogero RA: oneChannelGUI: a graphical interface to Bioconductor tools, designed for life scientists who are not familiar with R language. *Bioinformatics* 2007, 23:3406–3408
35. Bookout AL, Mangelsdorf DJ: Quantitative real-time PCR protocol for analysis of nuclear receptor signaling pathways. *Nucl Recept Signal* 2003, 1:e012
36. Gentleman RC, Carey VJ, Bates DM, Bolstad B, Dettling M, Dudoit S, Ellis B, Gautier L, Ge Y, Gentry J, Hornik K, Hothorn T, Huber W, Iacus S, Irizarry R, Leisch F, Li C, Maechler M, Rossini AJ, Sawitzki G, Smith C, Smyth G, Tierney L, Yang JY, Zhang J: Bioconductor: open software development for computational biology and bioinformatics. *Genome Biol* 2004, 5:R80
37. Breitling R, Armengaud P, Amtmann A, Herzyk P: Rank products: a simple, yet powerful, new method to detect differentially regulated genes in replicated microarray experiments. *FEBS Lett* 2004, 573:83–92
38. Sasson A, Michael TP: Filtering error from SOLiD Output. *Bioinformatics* 2010, 26:849–850
39. Rumble SM, Lacroite P, Dalca AV, Fiume M, Sidow A, Brudno M: SHRiMP: accurate mapping of short color-space reads. *PLoS Comput Biol* 2009, 5:e1000386
40. Robinson MD, Smyth GK: Small-sample estimation of negative binomial dispersion, with applications to SAGE data. *Biostatistics* 2008, 9:321–332
41. Perou CM, Sorlie T, Eisen MB, van de Rijn M, Jeffrey SS, Rees CA, Pollack JR, Ross DT, Johnsen H, Akslen LA, Fluge O, Pergamenschikov A, Williams C, Zhu SX, Lonning PE, Borresen-Dale AL, Brown PO, Botstein D: Molecular portraits of human breast tumours. *Nature* 2000, 406:747–752
42. Betel D, Koppal A, Agius P, Sander C, Leslie C: Comprehensive modeling of microRNA targets predicts functional non-conserved and non-canonical sites. *Genome Biol* 2010, 11:R90
43. Gilli F, Lindberg RL, Valentino P, Marnetto F, Malucchi S, Sala A, Capobianco M, di Sapio A, Sperli F, Kappos L, Calogero RA, Bertolotto A: Learning from nature: pregnancy changes the expression of inflammation-related genes in patients with multiple sclerosis. *PLoS One* 2010, 5:e8962
44. Smyth GK: Linear models and empirical bayes methods for assessing differential expression in microarray experiments. *Stat Appl Genet Mol Biol* 2004, 3: Article3
45. Calogero RA, Quaglino E, Saviozzi S, Forni G, Cavallo F: Oncoantigens as anti-tumor vaccination targets: the chance of a lucky strike? *Cancer Immunol Immunother* 2008, 57:1685–1694
46. Cho RW, Wang X, Diehn M, Shedden K, Chen GY, Sherlock G, Gurney A, Lewicki J, Clarke MF: Isolation and molecular characterization of cancer stem cells in MMTV-Wnt-1 murine breast tumors. *Stem Cells* 2008, 26:364–371
47. Jeter CR, Liu B, Liu X, Chen X, Liu C, Calhoun-Davis T, Repass J, Zaehres H, Shen JJ, Tang DG: NANOG promotes cancer stem cell characteristics and prostate cancer resistance to androgen deprivation. *Oncogene* 2011, 30:3833–3845
48. Hao JM, Chen JZ, Sui HM, Si-Ma XQ, Li GQ, Liu C, Li JL, Ding YQ, Li JM: A five-gene signature as a potential predictor of metastasis and survival in colorectal cancer. *J Pathol* 2010, 220:475–489
49. Yu K, Ganesan K, Tan LK, Laban M, Wu J, Zhao XD, Li H, Leung CH, Zhu Y, Wei CL, Hooi SC, Miller L, Tan P: A precisely regulated gene expression cassette potently modulates metastasis and survival in multiple solid cancers. *PLoS Genet* 2008, 4:e1000129
50. Klein U, Dalla-Favera R: New insights into the pathogenesis of chronic lymphocytic leukemia. *Semin Cancer Biol* 2010, 20:377–383
51. Hurst DR, Edmonds MD, Welch DR: Metastamir: the field of metastasis-regulatory microRNA is spreading. *Cancer Res* 2009, 69:7495–7498
52. Polyak K, Weinberg RA: Transitions between epithelial and mesenchymal states: acquisition of malignant and stem cell traits. *Nat Rev Cancer* 2009, 9:265–273
53. Urbich C, Kuehbach A, Dimmeler S: Role of microRNAs in vascular diseases, inflammation, and angiogenesis. *Cardiovasc Res* 2008, 79:581–588
54. Astolfi A, Rolla S, Nanni P, Quaglino E, De Giovanni C, Iezzi M, Musiani P, Forni G, Lollini PL, Cavallo F, Calogero RA: Immune prevention of mammary carcinogenesis in HER-2/neu transgenic mice: a microarray scenario. *Cancer Immunol Immunother* 2005, 54:599–610
55. Cavallo F, Calogero RA, Forni G: Are oncoantigens suitable targets for anti-tumour therapy? *Nat Rev Cancer* 2007, 7:707–713
56. Calogero RA, Quaglino E, Saviozzi S, Forni G, Cavallo F: Oncoantigens as anti-tumor vaccination targets: the chance of a lucky strike? *Cancer Immunol Immunother* 2008, 57:1685–1694
57. Li LN, Zhang HD, Zhi R, Yuan SJ: Down-regulation of some miRNAs by degrading their precursors contributes to anti-cancer effect of mistletoe lectin-I. *Br J Pharmacol* 2011, 162:349–364
58. Navarro A, Diaz T, Martinez A, Gaya A, Pons A, Gel B, Codony C, Ferrer G, Martinez C, Montserrat E, Monzo M: Regulation of JAK2 by miR-135a: prognostic impact in classic Hodgkin lymphoma. *Blood* 2009, 114:2945–2951
59. Wang YX, Zhang XY, Zhang BF, Yang CQ, Chen XM, Gao HJ: Initial study of microRNA expression profiles of colonic cancer without lymph node metastasis. *J Dig Dis* 2010, 11:50–54
60. Vickers MM, Bar J, Gorn-Hondermann I, Yarom N, Daneshmand M, Hanson JE, Addison CL, Asmis TR, Jonker DJ, Maroun J, Lorimer IA, Goss GD, Dimitroulakos J: Stage-dependent differential expression of microRNAs in colorectal cancer: potential role as markers of metastatic disease. *Clin Exp Metastasis* 2012, 29:123–132
61. Xu XM, Qian JC, Deng ZL, Cai Z, Tang T, Wang P, Zhang KH, Cai JP: Expression of miR-21, miR-31, miR-96 and miR-135b is correlated with the clinical parameters of colorectal cancer. *Oncol Lett* 2012, 4:339–345
62. Lulla RR, Costa FF, Bischof JM, Chou PM, de F Bonaldo M, Vanin EF, Soares MB: Identification of differentially expressed microRNAs in osteosarcoma. *Sarcoma* 2011, 2011:732690
63. Costa FF, Bischof JM, Vanin EF, Lulla RR, Wang M, Sredni ST, Rajaram V, Bonaldo Mde F, Wang D, Goldman S, Tomita T, Soares MB: Identification of microRNAs as potential prognostic markers in ependymoma. *PLoS One* 2011, 6:e25114
64. Liu S, Guo W, Shi J, Li N, Yu X, Xue J, Fu X, Chu K, Lu C, Zhao J, Xie D, Wu M, Cheng S: MicroRNA-135a contributes to the development of portal vein tumor thrombus by promoting metastasis in hepatocellular carcinoma. *J Hepatol* 2012, 56:389–396
65. Rovero S, Amici A, Di Carlo E, Bei R, Nanni P, Quaglino E, Porcedda P, Boggio K, Smorlesi A, Lollini PL, Landuzzi L, Colombo MP, Giovarelli M, Musiani P, Forni G: DNA vaccination against rat her-2/Neu p185 more effectively inhibits carcinogenesis than transplantable carcinomas in transgenic BALB/c mice. *J Immunol* 2000, 165:5133–5142
66. Lindow M, Gorodkin J: Principles and limitations of computational microRNA gene and target finding. *DNA Cell Biol* 2007, 26:339–351
67. Alexiou P, Maragkakis M, Papadopoulos GL, Reczko M, Hatzigeorgiou AG: Lost in translation: an assessment and perspective for computational microRNA target identification. *Bioinformatics* 2009, 25:3049–3055
68. Aranda-Orgilles B, Aigner J, Kunath M, Lurz R, Schneider R, Schweiger S: Active transport of the ubiquitin ligase MID1 along the

- microtubules is regulated by protein phosphatase 2A. *PLoS One* 2008, 3:e3507
69. Leibowitz-Amit R, Tsarfay G, Abargil Y, Yerushalmi GM, Horev J, Tsarfay I: Mimp, a mitochondrial carrier homologue, inhibits Met-HGF/SF-induced scattering and tumorigenicity by altering Met-HGF/SF signaling pathways. *Cancer Res* 2006, 66:8687–8697
70. Zaltsman Y, Shachnai L, Yivgi-Ohana N, Schwarz M, Maryanovich M, Houtkooper RH, Vaz FM, De Leonadis F, Fiermonte G, Palmieri F, Gillissen B, Daniel PT, Jimenez E, Walsh S, Koehler CM, Roy SS, Walter L, Hajnoczky G, Gross A: MTCH2/MIMP is a major facilitator of tBID recruitment to mitochondria. *Nat Cell Biol* 2010, 12:553–562